NANO · MICRO
small

Supporting Information

for *Small*, DOI 10.1002/smll.202303517

Tumor Vascular Destruction and cGAS-STING Activation Induced by Single Drug-Loaded Nano-Micelles for Multiple Synergistic Therapies of Cancer

Jingyu Gu, Xinpei Liu, Zhongfang Ji, Mengling Shen, Minqian Zhu, Yuanyuan Ren, Li Guo, Kai Yang, Teng Liu and Xuan Yi**

Supplementary Materials

Tumor Vascular Destruction and cGAS-STING Activation Induced by Single Drug-Loaded Nano-Micelles for Multiple Synergistic Therapies of Cancer

Jingyu Gu[1], Xinpei Liu[1], Zhongfang Ji[1], Mengling Shen[1], Minqian Zhu[1], Yuanyuan Ren[1], Li Guo[1], Kai Yang[2], Teng Liu[2]*, Xuan Yi[1]*

1. School of Pharmacy, Jiangsu Key Laboratory of Inflammation and Molecular Drug Targets, Nantong University, Nantong, Jiangsu, 226001, China.

2. State Key Laboratory of Radiation Medicine and Protection, School of Radiation Medicine and Protection and School for Radiological and Interdisciplinary Sciences (RAD-X), Collaborative Innovation Center of Radiation Medicine of Jiangsu Higher Education Institutions, Soochow University, Suzhou, Jiangsu, 215123, China.

* Correspondence should be sent to: xuanyi@ntu.edu.cn; tliu13@suda.edu.cn.

Materials and Methods

Materials

Polyethylene glycol grafted poly (lactic-co-glycolic) acid co-polymer (mPEG-PLGA), 50:50 (w:w), (Mw B5,000:10,000 Da) was purchased from Xi'an Ruixi Biotechnolog Co., Ltd. DMXAA (ASA404 , Vadimezan) was purchased from RHAWN. Dimethyl sulfoxide (DMSO) and acetonitrile were obtained from Sinopharm Chemical Reagent Co. Anti-PD-L1 was purchased from Bioxcell (Clone: 10F.9G2; Catalog#: BE0101). Flow cytometric antibodies of cell surface markers were obtained from eBioscience or elabscience. Enzyme-linked immunosorbent assay test kits were purchased from MultiSciences Biotech Co., Ltd or Jiangsu Meimian Industrial Co., Ltd. All of the schematic diagrams, including ToC, Figure 1a, 3a, 4g, 6b, 6d, 7a and 7f, had been created with BioRender.com with permission.

Functional verification of blood

To determine the UV-Vis-NIR light absorption of blood, the whole blood was collected from BALB/c female mice using anticoagulant tubes and diluted 200-fold, 400-fold, and 800-fold with anticoagulant, respectively. The UV-Vis-NIR absorption spectra of the diluted blood were measured. In order to investigate the photothermal conversion of blood under 808-nm laser exposure, the collected blood was prepared and irradiated with 808-nm laser for 8 min. The temperature changes were recorded with an infrared thermal imager (FLIR Systems Inc., FLIR E50, USA). To examine the release of oxygen from blood, blood was collected from BALB/c mice into anticoagulant tubes. Portable oximeters (Leici, JPBJ-608, China) were used to measure the amount and rate of oxygen release from the indicated solutions in 40 min.

The synthesis of PPD

PPD nanoparticles were obtained according to a simple synthesis method that has been reported. [1] Briefly, 60 μL DMXAA (2.5 mg/mL) in DMSO was added to 1 mL mPEG-PLGA (10 mg/mL) dissolved in acetonitrile. After sonication for 5 minutes, the mixture solution was dropwisely added to 5 mL of water. After stirring for 1 h and standing for 6 h, dialysis was performed for 6 h to remove organic solvent to obtain PPD nanoparticles.

Characterization of PPD Nanomicelles

The UV absorption of free DMXAA, PP and PPD was measured by UV-Vis-NIR spectrophotometer. The hydrodynamic sizes of PP and PPD was measured with dynamic light scattering (Malvern, Zetasizer Nano ZS90, UK). The concentration of DMXAA in PPD was

measured by UV–Vis absorption spectra of PPD and PP. The absorption spectra of PPD and PP were firstly fitted at 500 nm and then the difference value between the absorption of PPD and PP at 345 nm was brought into the standard curve of DMXAA to calculate the drug concentration.

Cell experiments

HUVEC cells (5×10^4 cells/well) were first pre-seeded on small discs in 24-well plates and then incubated with PPD-DID for 12 h. Subsequently, cells were fixed with 4% paraformaldehyde and subsequently stained with DAPI. The collected cells were analyzed by confocal microscopy (Olympus Corporation, Olympus FV1200, Japan). For cytotoxicity assessment, HUVEC cells were seeded into 96-well plate (8.0×10^3 cells per well). Afterwards, the cells were co-incubated with different concentrations of free DMXAA or PPD (DMXAA = 0 -75 μg/ml) for 24 h. Finally, CCK-8 assay were then performed to assess relative cell survival according to the standard protocol.

The analysis of tumor vascular destruction

Female BALB/c mice (6-8 weeks old) were uniformly ordered by Changzhou Kavins Experimental Animal Co. LTD. Animal feeding and management was performed according to the SOP of Laboratory Animal Center of Nantong University. All animal experiments were performed according to the experimental protocols approved by the Laboratory Animal Center of Nantong University. Murine breast cancer cells (4T1) were purchased from American Type Culture Collection (ATCC). 4T1 cells (2×10^6) were injected subcutaneously into the back of mice at a dose of 50 μL per mouse to construct a mouse subcutaneous tumor model. Tumor size was calculated by the formula: V = length × width × width/2 (mm^3). Mice were euthanized when the detected tumor volume exceeded 1000 mm^3.

Tumor tissues were collected from 4T1 tumor-bearing mice injected intravenously with PPD (10 mg DMXAA/kg) and stained with H&E. For detection of hemoglobin content in tumors, we collected the tumors from mice injected with PPD at appointed time. The tumors were weight and homogenized in 1 mL PBS. Red blood cell lysis buffer was then added and incubated at room temperature for 10 min to fully lyse red blood cells. Afterwards, the lysed samples were centrifuged (14,800 rpm, 10 min) and the absorbance of the supernatant was detected at 540 nm after discarding the pellet.

Photoacoustic imaging and photothermal therapy

The tumors of mice i.v. injected with PPD or PP were imaged by Vevo LAZR photoacoustic imaging system (VisualSonics, Vevo LAZR, Canada) at various time points (0, 2, 6, 12, and 24 h). We chose the tumor center region of the imaged mouse as the region of interest (ROI) and obtained the average tumor PA signal by calculation. At 12 h post i.v. injection of PPD, tumors were irradiated by 808-nm laser (0.8 W/cm^2, 8 min). An infrared camera was used to record the changed tumor temperature.

In vivo fluorescence imaging

To verify the tumor-targeting efficacy of PPD in 4T1 tumor-bearing mice, 4T1 tumor-bearing mice were injected with PPD-DID via the tail vein. In vivo imaging of mice was performed by an animal fluorescence imaging software IVIS system (PerkinElmer, IVIS® Lumina, USA) at various time points.

Distant tumor inhibition

In order to construct the bilateral tumor model, 4T1 cells (2×10^6) were injected subcutaneously into the right and left flanks of each mouse on the day -7 and -5, respectively. The tumor on the right flank was treated with PTT, RT (Rad source, RS-2000 Pro, USA) or surgery at day 0, and the size of the tumors on the left flank was measured.

Analysis of the proportion of immune cells

To analyze the proportion of DC maturation in lymph nodes and the proportion of various T cells in distant tumors, lymph nodes and 4T1 tumors collected from mice with indicated treatment were homogenized in PBS (pH 7.4) containing 1% FBS. The cells in lymph nodes were stained with FITC Anti-Mo CD11c (eBioscience, Clone: N418, 11-0114-82), APC Anti-Mo CD86 (eBioscience, Clone: GL1, 17-0862-82), PE Anti-Mo CD80 (eBioscience, Clone: 16-10A1, 12-0801-82) antibodies. The cells in tumor tissues were stained with FITC Anti-Mo CD3 (eBioscience, clone: 17A2, 11-0032-82), APC Anti-Mo CD4 (eBioscience, clone: GK1.5, 17-0041-83), PE Anti-Mo CD8a (eBioscience, clone: 53-6.7, 12-0081-83) antibodies according to the protocol to distinguish cytotoxic T lymphocytes (CTLs, $CD3^+CD4^-CD8^+$) and $CD4^+$ T cells ($CD3^+CD4^+CD8^-$). In order to analyze the proportion of Tregs in $CD4^+$ T cells, the cells were stained with FITC Anti-Mo CD3 (eBioscience, clone: 17A2, 11-0032-82), APC Anti-Mo CD4 (eBioscience, clone: GK1.5, 17-0041-83) and PE Anti-Mo Foxp3 (eBioscience, clone: NRRF-30, 12-4771-82). The cells were stained with Percp Anti-Mouse CD11b Antibody (elabscience, clone: M1/70, E-AB-F1081F) and FITC Anti-Mouse F4/80

Antibody (elabscience, clone: CI: A3-1, E-AB-F0995C), APC Anti-Mouse CD86 Antibody (elabscience, clone: 16-10A1, 12-0801-82) and PE Anti-Mouse CD206 Antibody (elabscience, clone: C068C2, E-AB-F1135D) to distinguish M1 and M2 macrophages. On 40^{th} day after treatment, the spleens were obtained from healthy mice or PPD-mediated therapies-treated mice, and stained with FITC Anti-Mo CD3 (eBioscience, clone: 17A2, 11-0032-82), PE Anti-Mo CD8a (eBioscience, clone: 53-6.7, 12-0081-83), APC Anti-Hu/Mo CD44 (eBioscience, clone: IM7, 17-0441-82) and PE-Cyanine7 Anti-Mo CD62L (eBioscience, clone: MEL-14, 25-0621-82) antibodies. $CD3^+CD8^+CD62L^-CD44^+$ cells were belonged to $CD8^+$ effector memory T cells (T_{EM}).

The inhibition of metastasis and recurrence

For the systemic metastasis model, 50 μL luciferase-4T1 cells (2×10^6) were first injected into the mammary pad of mice, and 200 μL luciferase-4T1 cells (4×10^5) in PBS were injected into mice by tail vein injection 5 days later. The primary tumors in the mice were eliminated by surgery or PPD-mediated therapies. Bioluminescence imaging was performed using an animal fluorescence imaging software IVIS system (PerkinElmer, IVIS® Lumina, USA). Potassium fluorescein salt substrate was injected intraperitoneally ten minutes prior to bioluminescence imaging in mice.

For the recurrence model, mice after treatment with PPD-mediated therapies and healthy mice were subcutaneously injected 4T1 cells (1×10^6) on day 40. The volumes of these subcutaneous tumors in each group were then measured.

Statistical analysis

The data were expressed as mean ± SD or S.E.M.. All statistical analyses were performed using GraphPad Prism 7.0/9.0 (GraphPad Software Inc. USA). Statistical analysis was performed by using a two-tailed Student's t-test for two groups. P values < 0.05 were considered statistically significant (*$P < 0.05$, **$P < 0.01$, ***$P < 0.001$, and ****$P < 0.0001$). The detailed statistical description, including sample size (n) and statistical method, was showed in each figure caption.

References

[1] Q. Chen, L. Xu, C. Liang, C. Wang, R. Peng, Z. Liu, Nat. Commun. 2016, 7, 13193.

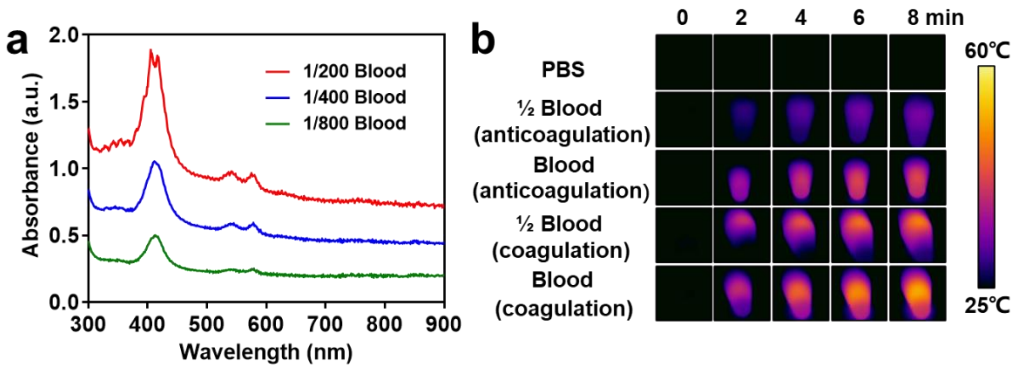

Figure S1: (a) UV-Vis-NIR absorption spectroscopy of blood at different diluted concentrations. (b) Infrared images obtained with PBS, coagulated blood, anti-coagulated blood exposed to 808-nm laser for 8 minutes.

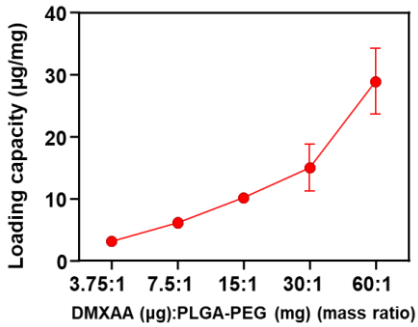

Figure S2: DMXAA loading capacity of PP at different mass ratio of DMXAA to PP. Data are presented as Mean ± SD, n=3.

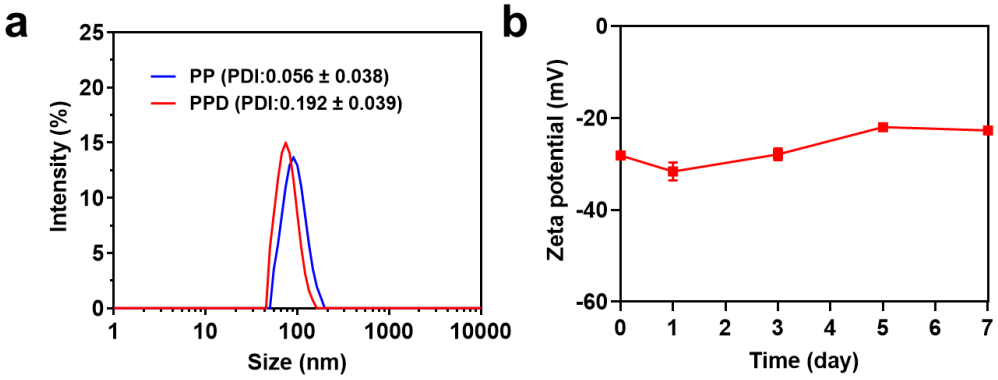

Figure S3: (a) Hydrodynamic sizes of PP and PPD in water. (b) Zeta potential of PPD in water during one week. Data are presented as Mean ± SD, n=3.

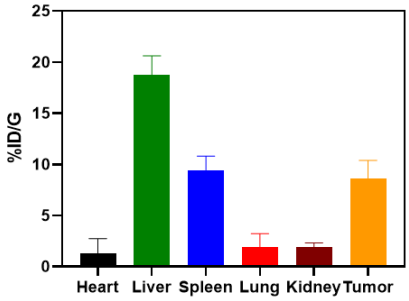

Figure S4: The bio-distribution of DID at 12 hours post intravenous injection of PLGA-PEG/DID&DMXAA. Data are presented as Mean ± SD, n=3.

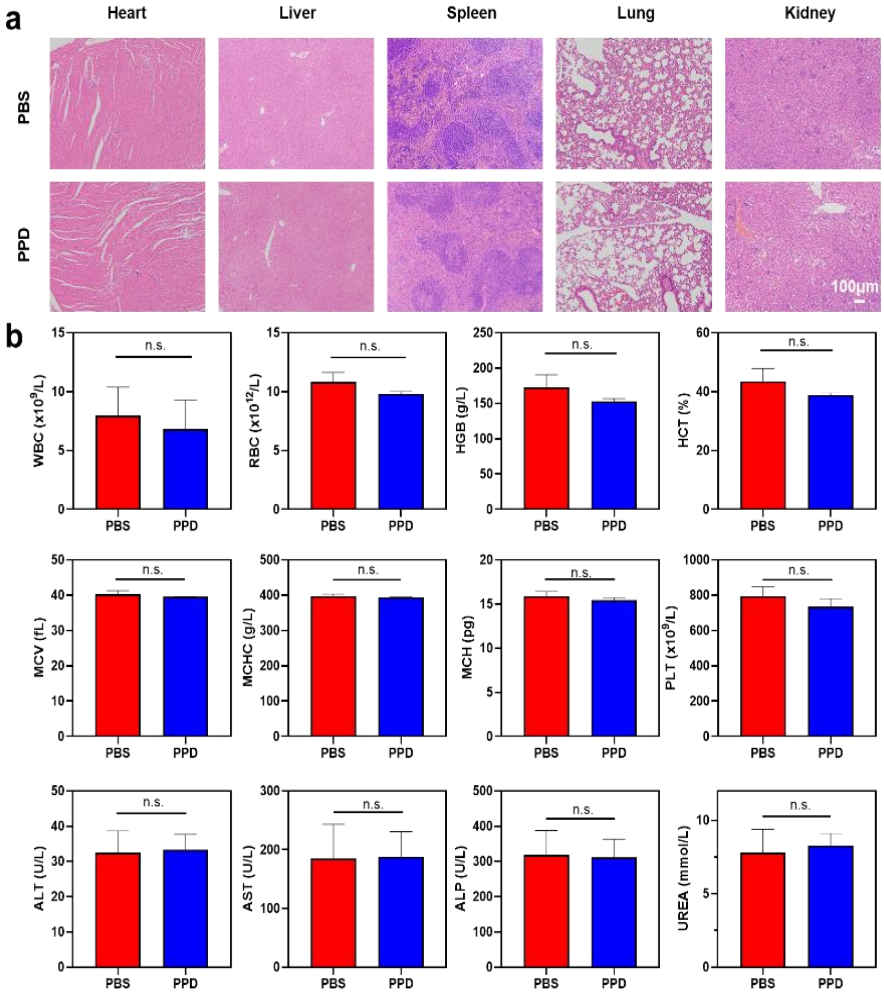

Figure S5: (a) H&E staining images of organs including heart, liver, spleen, lung and kidney collected from mice treated with PBS or PPD one day post injection (10 mg/kg of DMXAA). (b) Blood routine and blood biochemistry assay (including white blood cells (WBC), red blood cells (RBC), hemoglobin (HGB), hematocrit (HCT), mean corpuscular volume (MCV), mean corpuscular hemoglobin concentration (MCHC), mean corpuscular hemoglobin (MCH), platelets (PLT), alanine aminotransferase (ALT), aspartate aminotransferase (AST), alkaline phosphatase (ALP) and blood urea (UREA) levels of healthy female Balb/c mice treated with PBS or PPD one day post injection (10 mg/kg of DMXAA). P-values were calculated by Student's t-test (two-tailed) (Data are presented as Mean ± SD, n=3, n.s., non-significant).

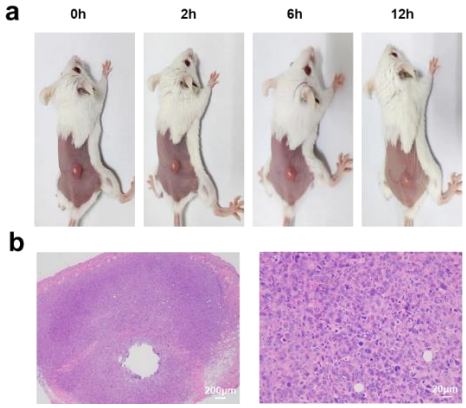

Figure S6: (a) Photographs of mice at 0, 2, 6 and 12 h after the injection with free DMXAA (10 mg/kg, dissolved in 5% $NaHCO_3$). (b) Representative images of H&E stained tumor slices collected from mice injected with free DMXAA.

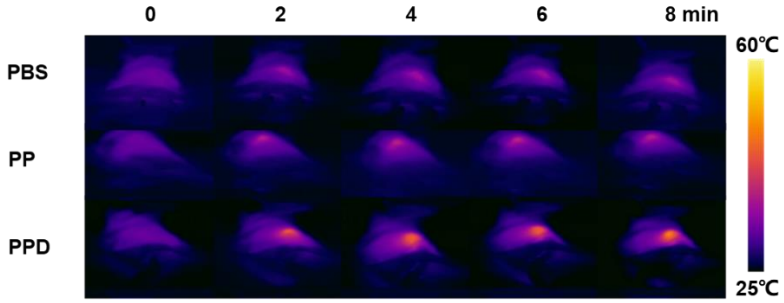

Figure S7: Representative IR thermal images of the tumor-bearing mice injected with PBS, PP and PPD under 808-nm laser irradiation.

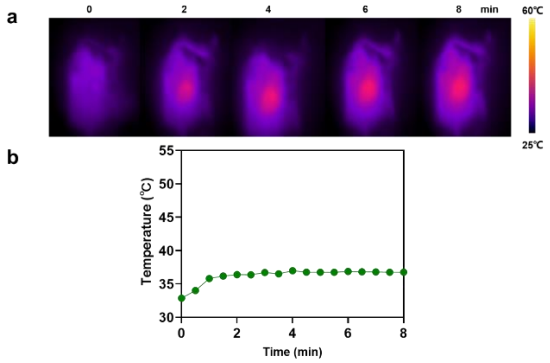

Figure S8: (a) Representative IR thermal images of the tumor-bearing mice injected with free DMXAA under 808-nm laser irradiation. (b) The temperature of tumor on mice 12 hours post i.v. injection of free DMXAA (10 mg/kg, dissolved in 5% $NaHCO_3$) under 808-nm laser exposure.

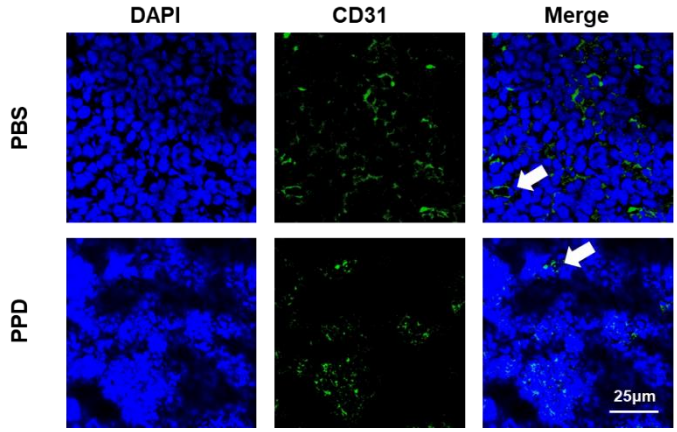

Figure S9: The tumor vessels were stained by CD31 antibody in untreated and PPD-treated tumors.

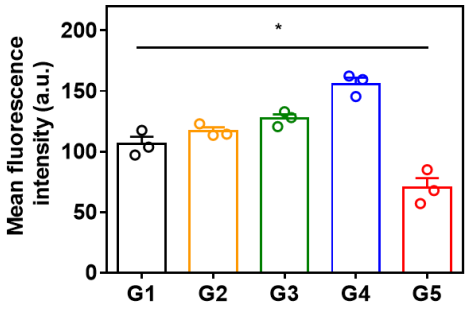

Figure S10: Semiquantitative analysis of tumor hypoxia. G1: PBS injection; G2: 12 hours post PPD injection; G3: 24 hours post PPD injection; G4: 72 hours post PPD injection; G5: 12 hours post PPD injection plus 808-nm laser irradiation. P-values were calculated by Student's t-test (two-tailed) (Data are presented as Mean ± S.E.M., n=3, *P <0.05).

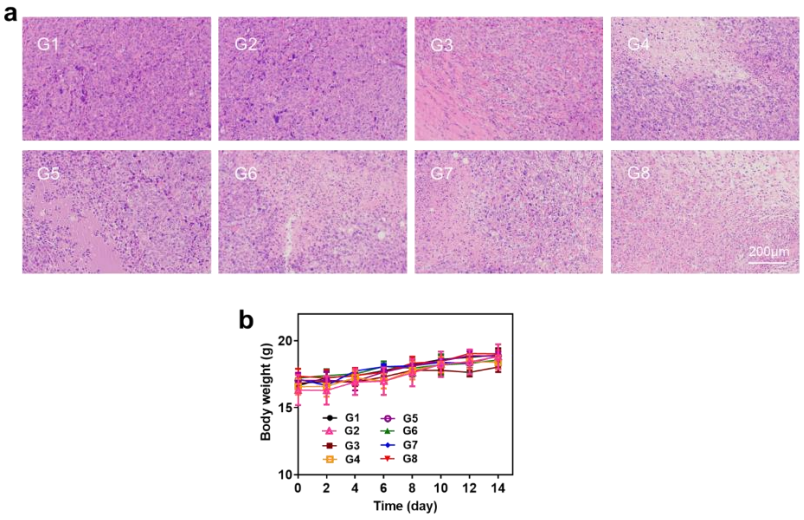

Figure S11: (a) H&E staining of distant tumor sections with various treatments. Scale bar = 200 μm. (b) Average body weights of 4T1 tumors-bearing mice with different treatments (Data are presented as Mean ± S.E.M., n=5). G1: PBS injection; G2: Laser exposure; G3: PPD injection; G4: X-rays exposure; G5: PP injection + Laser exposure + X-rays exposure; G6: PPD injection + Laser exposure; G7: PPD injection + X-rays exposure; G8: PPD injection + Laser exposure + X-rays exposure.

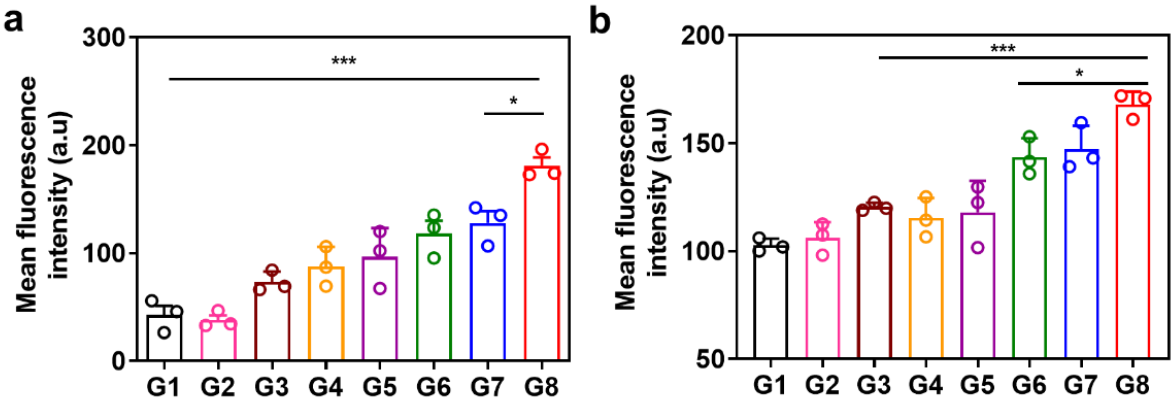

Figure S12: Semiquantitative analysis of CRT (a) /p-STING (b) immunofluorescence staining of primary tumors at day 2 post treatment. G1: PBS injection; G2: Laser exposure; G3: PPD injection; G4: X-rays exposure; G5: PP injection + Laser exposure + X-rays exposure; G6: PPD injection + Laser exposure; G7: PPD injection + X-rays exposure; G8: PPD injection + Laser exposure + X-rays exposure. P-values were calculated by Student's t-test (two-tailed) (Data are presented as Mean ± SD, n=3, *P < 0.05, ***P < 0.001).

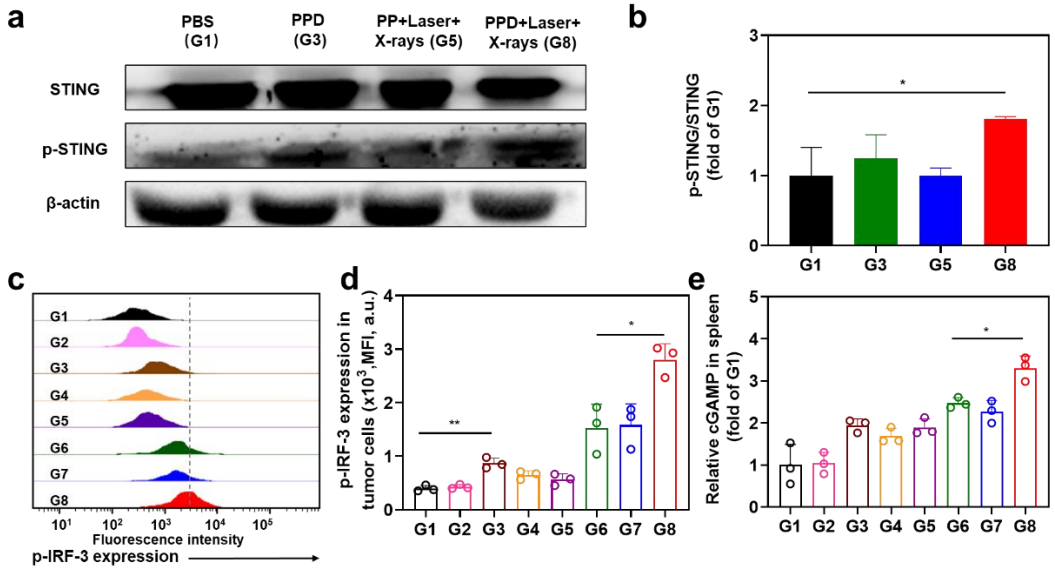

Figure S13: Representative western blotting images (a) and statistical analysis (b) of the expression of p-STING/STING in tumor tissues with the indicated treatments. Representative flow cytometry profiles (c) and statistical analysis (d) of the expression of p-IRF-3 in tumor tissues with indicated treatments. (e) The content of cGAMP in spleens collected from mice with the indicated treatments. G1: PBS injection; G2: Laser exposure; G3: PPD injection; G4: X-rays exposure; G5: PP injection + Laser exposure + X-rays exposure; G6: PPD injection + Laser exposure; G7: PPD injection + X-rays exposure; G8: PPD injection + Laser exposure + X-rays exposure. P-values were calculated by Student's t-test (two-tailed) (Data are presented as Mean ± SD, n=3, *P < 0.05, **P < 0.01).

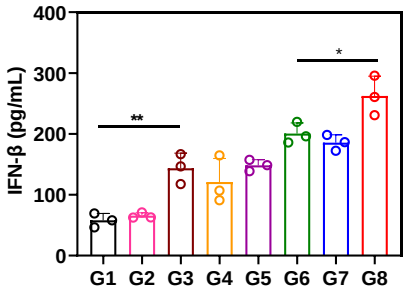

Figure S14: Cytokine secretion levels of IFN-β in serum collected from mice with different treatments at day 2. G1: PBS injection; G2: Laser exposure; G3: PPD injection; G4: X-rays exposure; G5: PP injection + Laser exposure + X-rays exposure; G6: PPD injection + Laser exposure; G7: PPD injection + X-rays exposure; G8: PPD injection + Laser exposure + X-rays exposure. P-values were calculated by Student's t-test (two-tailed) (Data are presented as Mean ± SD, n=3, *P < 0.05 and **P <0.01).

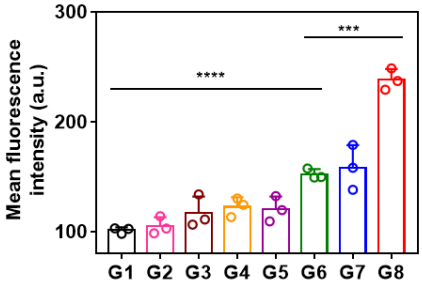

Figure S15: Semiquantitative analysis of p-STING immunofluorescence staining of distant tumors at day 7 post treatment. G1: PBS injection; G2: Laser exposure; G3: PPD injection; G4: X-rays exposure; G5: PP injection + Laser exposure + X-rays exposure; G6: PPD injection + Laser exposure; G7: PPD injection + X-rays exposure; G8: PPD injection + Laser exposure + X-rays exposure. P-values were calculated by Student's t-test (two-tailed) (Data are presented as Mean ± SD, n=3, ***P < 0.001, ****P < 0.0001).

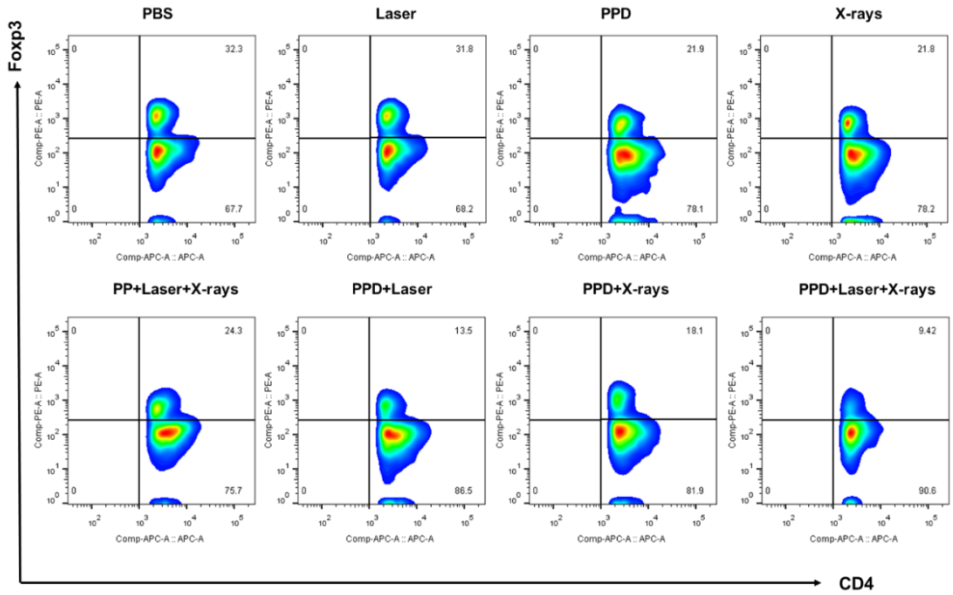

Figure S16: The representative flow cytometric profiles of $CD4^{+}Foxp3^{+}$ Tregs in tumors on day 7 after different treatments.

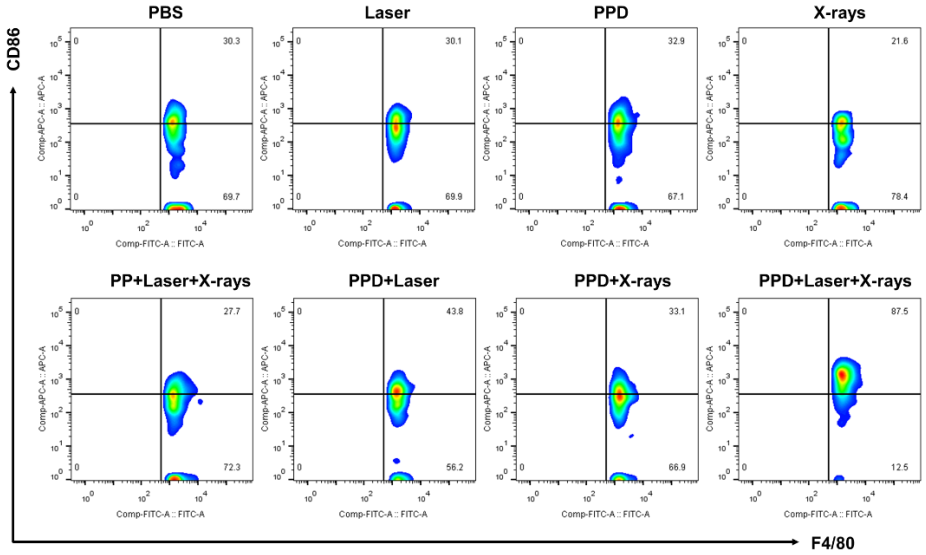

Figure S17: The representative flow cytometry profiles of M1 macrophages ($CD11b^{+}F4/80^{+}CD86^{+}$) in distant tumors on day 7 after different treatments.

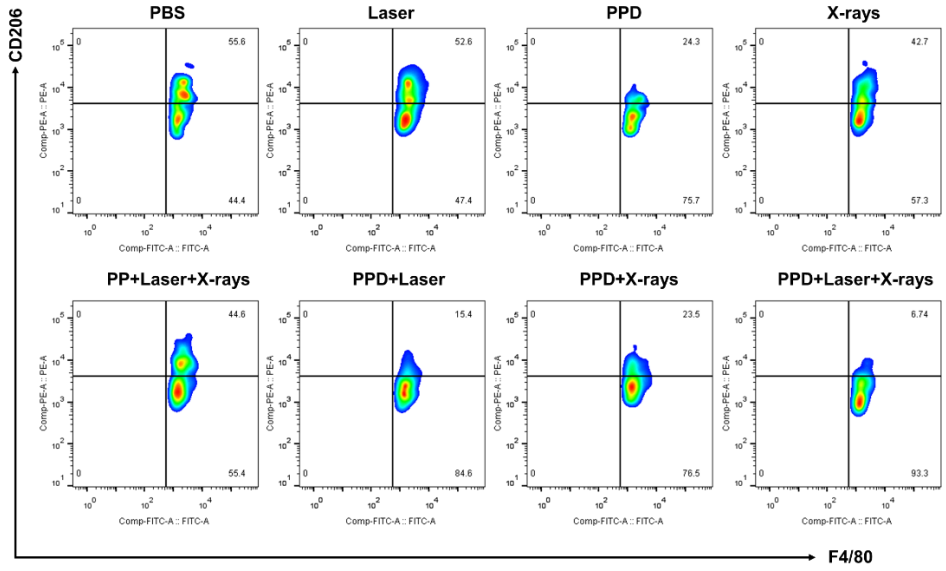

Figure S18: The representative flow cytometry profiles of M2 macrophages ($CD11b^{+}F4/80^{+}CD206^{+}$) in distant tumors on day 7 after different treatments.

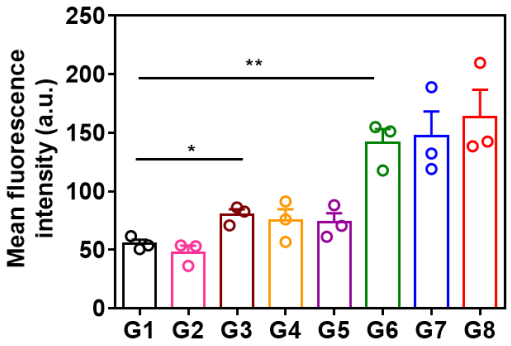

Figure S19: Semiquantitative analysis of immunofluorescence staining of PD-L1. G1: PBS injection; G2: Laser exposure; G3: PPD injection; G4: X-rays exposure; G5: PP injection + Laser exposure + X-rays exposure; G6: PPD injection + Laser exposure; G7: PPD injection + X-rays exposure; G8: PPD injection + Laser exposure + X-rays exposure. P-values were calculated by Student's t-test (two-tailed) (Data are presented as Mean ± S.E.M., n=3, *P < 0.05, **P <0.01).

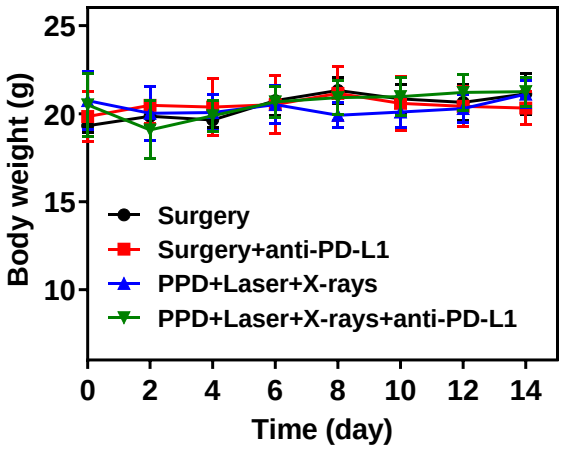

Figure S20: Average body weights of 4T1 tumors-bearing mice with different treatments (Data are presented as Mean ± SD, n = 5).